Progress In Electromagnetics Research B, Vol. 87, 19–38, 2020

Four-Port Rectangular Monopole Antenna for UWB-MIMO Applications

Watcharaphon Naktong and Amnoiy Ruengwaree*

Abstract—This paper proposes a four-port rectangular monopole antenna for ultra-wideband multiple-input multiple-output (UWB-MIMO) applications. The proposed antenna was designed by using step etching on the ground plane and arrow-shaped slot etching on a radiating patch to enhance bandwidth and improve performances. The homogeneous elements and angular variation techniques were applied to reduce mutual coupling between multiple antenna elements. The structural simulation technique used Computer Simulation Technology (CST) program to analyze the antenna characteristics such as reflection coefficient, group delay, mutual coupling, envelope correlation coefficient, and radiation patterns. The measured results were found to cover a frequency range of 3.1–10.6 GHz for UWB communications. The envelope correlation coefficient for the MIMO system was obtained under 0.001 which is less than the specific parameters of UWB-MIMO antennas. The radiation pattern was bi-directional. Also, the efficiency of the four-port antenna was more than 85.70%.

1. INTRODUCTION

The world's first wireless communication system had one antenna on both the transmitter and receiver. It is called Single-Input-Single-Output (SISO). It had been used since the birth of radio technology. However, the SISO system is limited in its performances. There are impact systems from interference and fading, then a system which uses a single antenna at the transmitter and multiple antennas at the receiver named as Single Input Multiple Output (SIMO) and a system which uses multiple antennas at the transmitter and a single antenna at the receiver called a Multiple Input Single Output (MISO) were presented. These had been developed to improve communication performances. Presently, Multiple-Input Multiple-Output (MIMO) communications system uses multiple antennas at both the transmitter and receiver. It has significantly enhanced the performances such as the data rate transmission speed, channel capacity improvement, and multipath fading reduction [1, 2].

However, the MIMO antenna is placed in multiple elements together to affect electromagnetic interactions between elements and high mutual coupling. The mutual coupling influences multiple elements antenna. A high mutual coupling can lead to impedance mismatches, increase the antenna correlation, decrease the efficiency of the antenna, etc. In the past years, researchers have studied techniques to reduce mutual coupling in multiple elements antenna for MIMO antenna. Some commonly used techniques include electromagnetic band-gap (EBG), inserting short stub, defected ground structure (DGS), spatial and angular variations, homogenous element, etc. [3–13].

This paper proposes a four-port rectangular monopole antenna for the UWB-MIMO application. In previous researches [14–20], a rectangle monopole antenna with step etching technique on a ground plane [21–23] was selected for an antenna structure to design the UWB-MIMO antenna [24], but it had some parameters that were not acceptable for the slot etching technique on radiating patch with

Received 29 October 2019, Accepted 14 January 2020, Scheduled 17 March 2020
* Corresponding author: Amnoiy Ruengwaree (amnoiy.r@en.rmutt.ac.th).
The authors are with the Department of Electronics and Telecommunication Engineering, Faculty of Engineering, Rajamangala University of Technology Thanyaburi (RMUTT), Pathumthani 12110, Thailand.

arrow-shaped improvement [14]. After that, it was designed into a two-port antenna placed in four different positions for a MIMO antenna as defined by the Federal Communication Commission (FCC). The orthogonal position is the best for performance [15] and antenna characteristics [25–28]. The homogeneous elements and angular variation techniques were applied to the four-port antenna for the inclination of mutual coupling and augmentation of the envelope correlation coefficient [29–34].

2. SINGLE PORT ANTENNA DESIGN

2.1. Single Port Antenna Design

In previous researches, the radiating patch antenna was designed with rectangular, triangular, and circular shapes with step-shaped etching on the ground plane to enhance the bandwidth. The rectangular shape is a proper shape for the UWB antenna for a single port [13]. The proposed structure of a single antenna was designed on a print circuit board (PCB) with FR4. The PCB had a dielectric constant value (ε_r) of 4.3, copper thickness (t) of 0.017 mm, and substrate thickness (h) of 0.764 mm.

The antenna structure was designed by using Eqs. (1)–(15) at a resonant frequency. The first step is to calculate the width at W and length at L, of the radiator patch with Eqs. (1)–(4) for [16, 17].

The width (W) of the patch was computed by

$$W = \frac{c}{2f_r}\sqrt{\frac{2}{\varepsilon_r + 1}}, \tag{1}$$

The effective dielectric constant was calculated by

$$\varepsilon_{eff} = \frac{\varepsilon_r + 1}{2} + \frac{\varepsilon_r - 1}{2}\left(\frac{1}{\sqrt{1 + \dfrac{2h}{W}}}\right), \tag{2}$$

The fringing fields resulting in the change in length was calculated by

$$\Delta L = 0.412h\frac{(\varepsilon_{eff} + 0.3)\left(\dfrac{W}{h} + 0.264\right)}{(\varepsilon_{eff} - 0.258)\left(\dfrac{W}{h} + 0.8\right)}, \tag{3}$$

The length (L) of the patch was calculated by

$$L = \frac{c}{2f_r\sqrt{\varepsilon_{eff}}} - 2\Delta L, \tag{4}$$

The second step was to design the feed line. The impedance of transmission line of antenna was fed by a coplanar waveguide for standard of 50 Ω and calculated by Eqs. (5)–(12) [18, 19].

The width W_f and length L_f of feed line were calculated as

$$W_f = \frac{0.07 * c}{f_r\sqrt{\varepsilon_{eff}}}, \tag{5}$$

$$L_f = \frac{0.3 * c}{f_r\sqrt{\varepsilon_{eff}}}, \tag{6}$$

where $K1$ and $K2$ are

$$K_1 = \frac{a}{b}; \quad a = \frac{W_f}{2}, \quad b = \frac{(2g + W_f)}{2}, \tag{7}$$

$$K_2 = \frac{\sinh\left(\dfrac{\pi a}{2h}\right)}{\sinh\left(\dfrac{\pi b}{2h}\right)}, \tag{8}$$

where

$$K' = \sqrt{1-(k)^2}, \tag{9}$$

$$q = \frac{1}{2}\left[\frac{K(k_2)}{K'(k_2)}\frac{K'(k_1)}{K(k_1)}\right] \tag{10}$$

$$\varepsilon_{re} = 1 + q(\varepsilon_r - 1), \tag{11}$$

$$Z_o = \frac{30\pi}{\sqrt{\varepsilon_{re}}} \times \frac{K'(k_1)}{K(k_1)} \tag{12}$$

By the way, the width $W1$ and length $L1$ of ground plan were obtained by Eqs. (13)–(14) [15, 17]

$$W_1 = \frac{0.32 * c}{f_r\sqrt{\varepsilon_{eff}}}, \tag{13}$$

$$L_1 = \frac{0.28 * c}{f_r\sqrt{\varepsilon_{eff}}}, \tag{14}$$

Finally, the width and length of substrate FR4 were calculated by Eq. (15) where $W_s = L_s \approx 34\,\text{mm}$ [15, 17]

$$W_S = L_S = 6h + W, \tag{15}$$

2.2. Design and Optimization of the Radiator Patch Antenna

The calculated parameters of the antenna design were width $(W) \approx 30\,\text{mm}$ and length $(L) \approx 22\,\text{mm}$ at a resonant frequency of 3.1 GHz. The simulation was performed using CST Microwave studio program. Therefore, in this section the radiator patch was optimized in [20] to enhance the impedance bandwidth into 2 steps. The first step was fixing the length value, L, to 22 mm and then decreasing the width, W to 30, 27, 24, 21, and 18 mm, respectively. The comparison of reflection coefficients is shown in Fig. 1. It was noticed that the suitable width, W, was 21 mm, and impedance bandwidth was between 2.49 and 5.23 GHz (70.98%), but it was not covered in frequency range of UWB as required.

So, the second step was to optimize by fixing the width, W, to 21 mm then adjusting the length, L, to 22, 20, 18, 16, and 14 mm, respectively. The comparison of simulated results is shown in Fig. 2. It

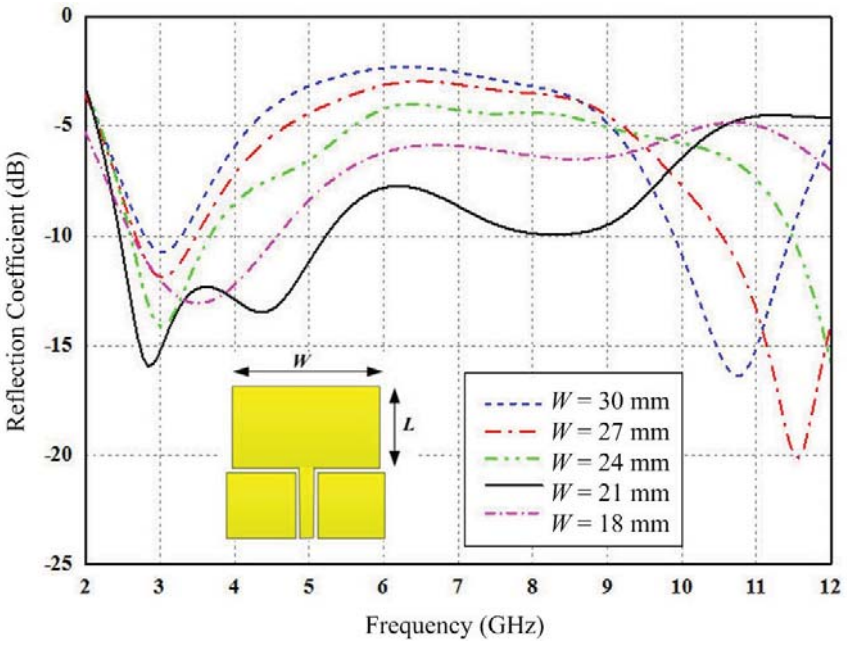

Figure 1. Comparison of reflection coefficients with optimization of W.

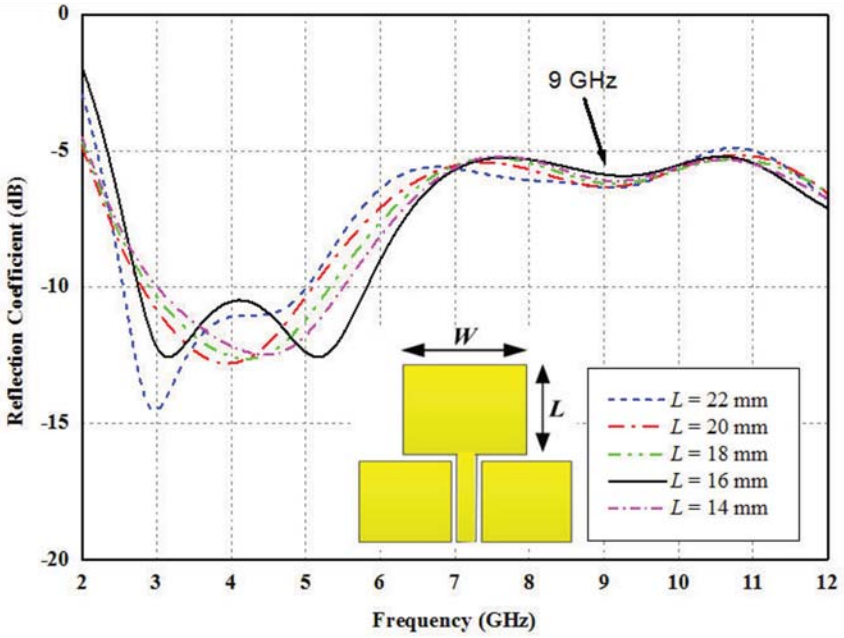

Figure 2. Comparison of reflection coefficients with optimization of L.

was observed that the appropriate value of L was 16 mm, and W was 21 mm. The impedance bandwidth was in frequency range of 2.77–5.93 GHz (72.64%), but it was still not covered in UWB communication system as defined by the Federal Communication Commission (FCC) [24]. Therefore, the conventional antenna will be designed in the next section.

2.3. Frequency Bandwidth Enhancement

This section presents the process for enhancing frequency bandwidth. From the appropriated result that $L = 16$ mm and $W = 21$ mm, it was found that the frequency range was between 5.93 and 12 GHz, and still got high reflection coefficient. There are 3 steps in order to improve and enhance bandwidth to cover the UWB. In the first step, observing the current distribution at 9 GHz was needed to be analyzed as shown in Fig. 3(a). It was observed that high current distributed at points A, B, and C on the ground plane. Consequently, using the slot etching technique on the ground plane [22, 23] at points A and B was presented when $W2$ and $L2$ were 6 mm and 3 mm, respectively. The presented antenna was shown in Fig. 3(b) and referred to as antenna type I. It was observed that the bandwidth was wider in dual-band frequency at 2.72–7.13 GHz (89.54%) and 7.76–11.77 GHz (41.07%). Fig. 4 shows the comparison

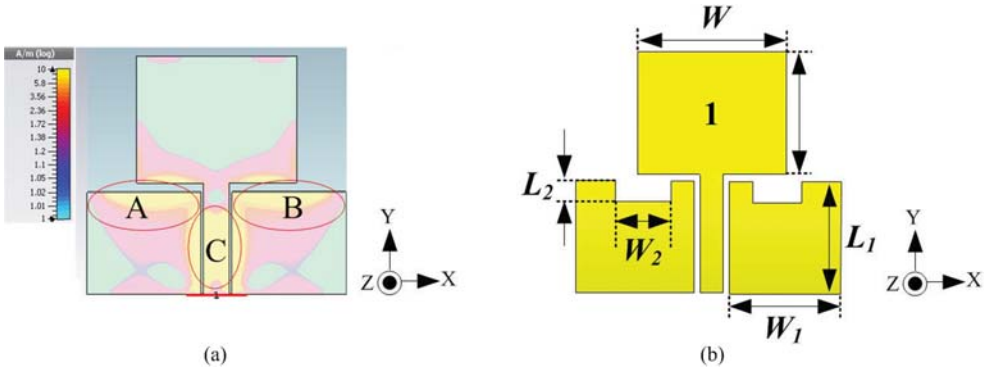

Figure 3. (a) The current distribution at 9 GHz, (b) the structure of antenna type I.

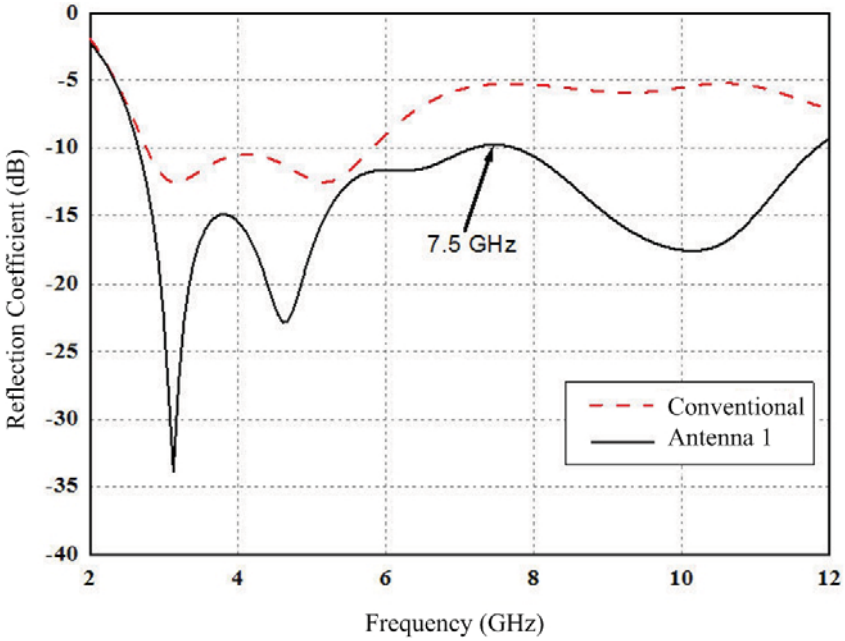

Figure 4. Comparison of simulations for conventional and antenna type I.

between conventional patch antenna and antenna type I. It portrays that the reflection coefficient was still high around 7.5 GHz, and impedance bandwidth was not covered in the UWB frequency range of 3.1–10.6 GHz.

Figure 5(a) shows the current distribution at 7.5 GHz, and it was overcrowding at the outer edge of ground planes. Then the second proposed step was to reduce the current distribution by using the slot etching technique on the ground plane again at points D and E with W_3 of 5 mm and L_3 of 2 mm and represented to be antenna type II as shown in Fig. 5(b).

Group delay is one of the important parameters of transmitting time of the amplitude envelopes of various sinusoidal components of UWB signals through a device. It effectively propagated delay in transmitting antenna (Tx) and receiving antenna (Rx) together; the group delay value must be less than ±2 ns as a specific for UWB-MIMO antenna [24]. The slot etching technique with an arrow-shaped slot was used on radiating patch to improve performance in [14], existing when $W4$ was 3 mm; $L4$ was 4 mm; $W5$ was 7 mm; and $L5$ was 8 mm as shown in Fig. 5(c), and it was named antenna type III. It was found in simulated results between antenna type II and antenna type III that the reflection coefficients had a small

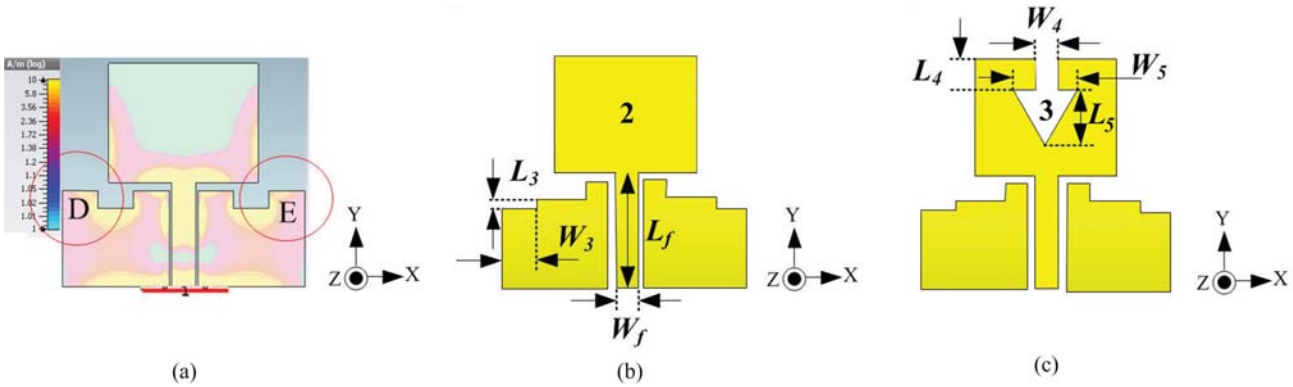

Figure 5. The process design of the single port antenna. (a) Current distribution at 7.5 GHz. (b) Antenna type II. (c) Antenna type III.

difference during the operating frequency range of 2.62–12 GHz (128.32%) and 2.63–12 GHz (128.09%) respectively as show in Fig. 6, when the distance between antenna under test as transmitted antenna and received antenna was varied of 10 cm, 20 cm, 30 cm, 40 cm, and 50 cm, respectively. It seems that suitable efficiency has occurred at a distance of 30 cm, applied for pulse signal transmission, but the group delay decreases less ± 2 ns as shown in Fig. 7. Etching a copper layer in step shape on the ground plane and arrow-shaped slot on a radiating patch were used to enhance bandwidth and improve performances of antenna characteristic as shown in Fig. 8. The homogeneous elements and angular variation techniques were applied to reduce mutual coupling between multiple antenna elements. The structural simulation

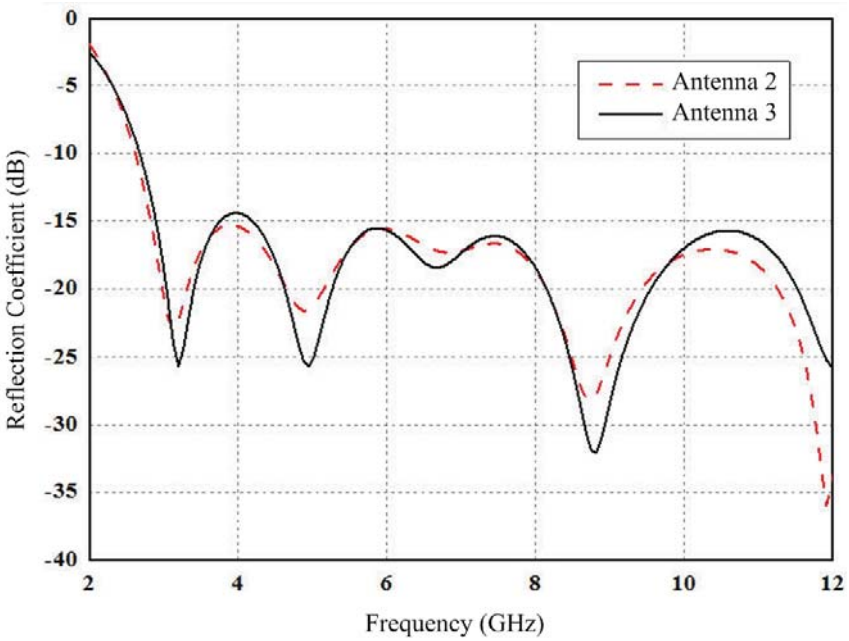

Figure 6. The comparison of reflection coefficients between antenna type II and antenna type III.

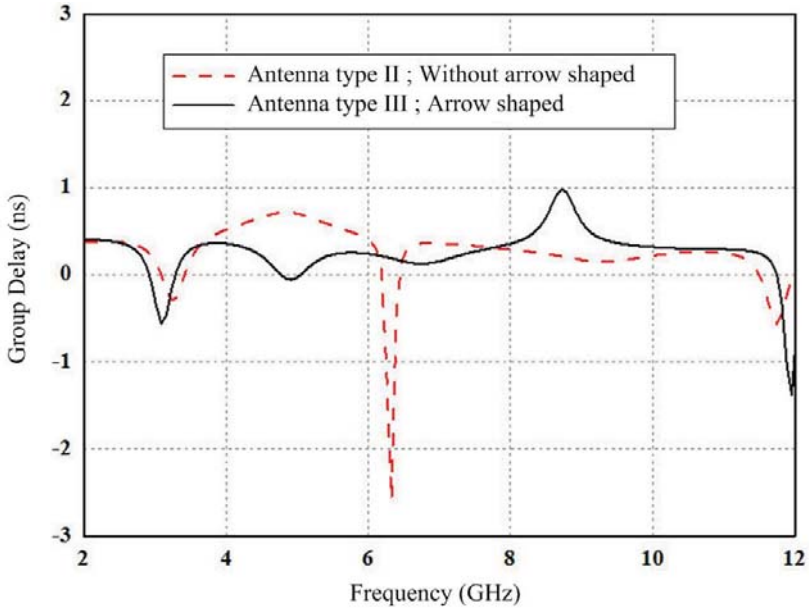

Figure 7. The comparison of simulation for group delay.

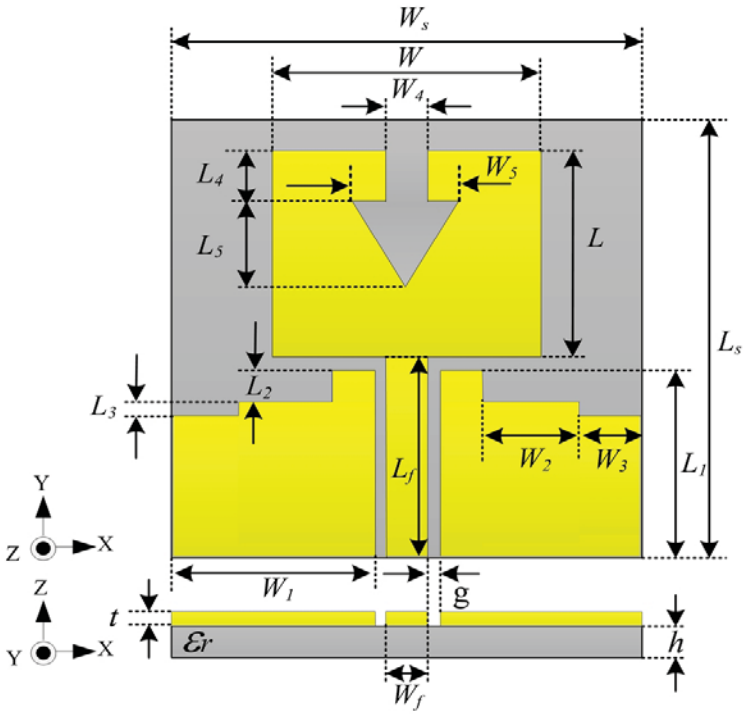

Figure 8. The prototype of single port antenna structure.

technique used CST program to analyze the antenna characteristics such as reflection coefficient, group delay, mutual coupling, envelope correlation coefficient, and radiation patterns. The measured results were found to cover a frequency range of 3.1–10.6 GHz for UWB communications.

The proper size of an effective antenna are with the following parameters of the reflection coefficient values and bandwidth: $L_S = 34\,\text{mm}$, $L = 16\,\text{mm}$, $L_f = 14\,\text{mm}$, $L_1 = 13\,\text{mm}$, $L_2 = 3\,\text{mm}$, $L_3 = 2\,\text{mm}$, $L_4 = 4\,\text{mm}$, $L_5 = 8\,\text{mm}$ and widths of $W_S = 34\,\text{mm}$, $W = 21\,\text{mm}$, $W_f = 3.2\,\text{mm}$, $W_1 = 15.1\,\text{mm}$, $W_2 = 6\,\text{mm}$, $W_3 = 5\,\text{mm}$, $W_4 = 3\,\text{mm}$, $W_5 = 7\,\text{mm}$ and $g = 0.3\,\text{mm}$, respectively, as shown in Fig. 8.

3. TWO PORT ANTENNAS DESIGN

3.1. Element Spacing and Placing Position

The single port antenna was selected at the frequency centered at 6.85 GHz (3.1–10.6 GHz) to design the array with antenna ports (1×2) for supporting the UWB-MIMO systems. The signal was transmitted by multiple elements of antenna which was generally supposed to be independent. The mutual coupling and isolation are significant effects for individuality between antenna elements. Therefore, the distance between antenna elements must be analyzed. In [25], the distances between antenna elements of $\lambda/2$, $\lambda/4$, and $\lambda/8$ were studied. It was observed that the distances of $\lambda/2$ and $\lambda/4$ had low correlation coefficient. For a narrow spacing of $\lambda/8$, the overall correlation coefficient was the highest. In previous researches, there were many techniques for reducing mutual coupling and enhancing isolation such as electromagnetic band-gap (EBG), insertion of short stub, defect ground structure (DGS), spatial and angular variations, and homogenous element [3–12]. In this session, the homogeneous elements and angular variation techniques were applied to improve performance of a UWB-MIMO antenna. So, the two-port antenna was optimized maintaining the same dimension structure without inserting any addition structures.

In [15], it was designed by placing a rectangular patch antenna with four different angular positions as shown in Fig. 9. The appropriate distances between ports were considered based on the value of mutual coupling. The mutual coupling was observed by correlation coefficients of S_{21} and S_{12} which

were not more than −15 dB as a specification required by the UWB-MIMO antenna [24]. The aim is to design a compact size antenna. So, the distance (d) of the edge of each antenna element should be equal to $\lambda/2$ (0.5λ) as shown in Fig. 9. Fig. 10 shows the comparison of mutual coupling of the spacing adjustment, d, of the two patch antennas whose orthogonal position is the best of mutual coupling as shown in Fig. 9(b). When the distance was varied from 0.50λ to 0.40λ, 0.30λ, and 0.25λ, it was observed that between port 1 and port 2 of each antenna could not be set less than 0.25λ, because the antenna structure would overlap on the ground plane and form a high mutual coupling as shown at point A of

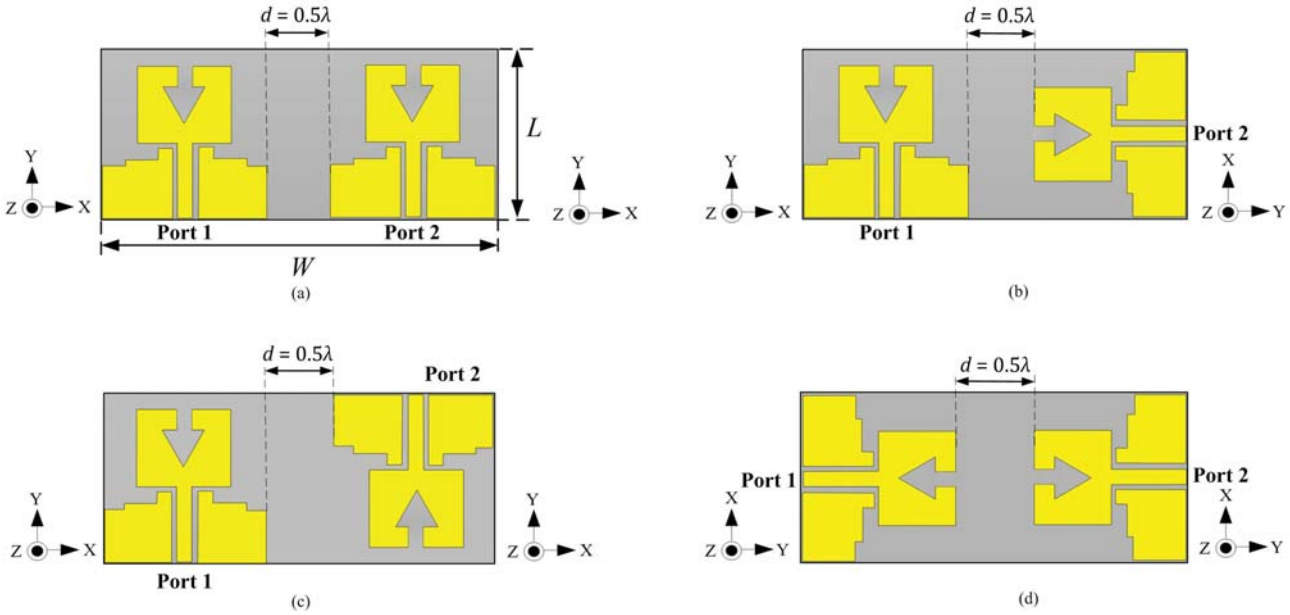

Figure 9. Placing the patch antenna in four different angular positions: (a) Side by side, (b) orthogonal, (c) parallel and (d) front by front.

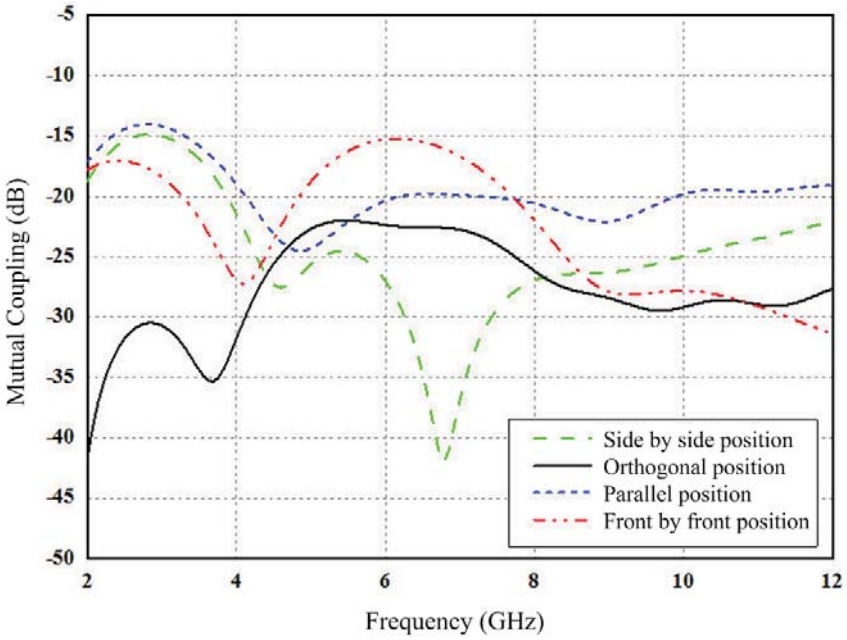

Figure 10. The simulation mutual coupling of four difference angular positions when $d = 0.50\,\lambda$.

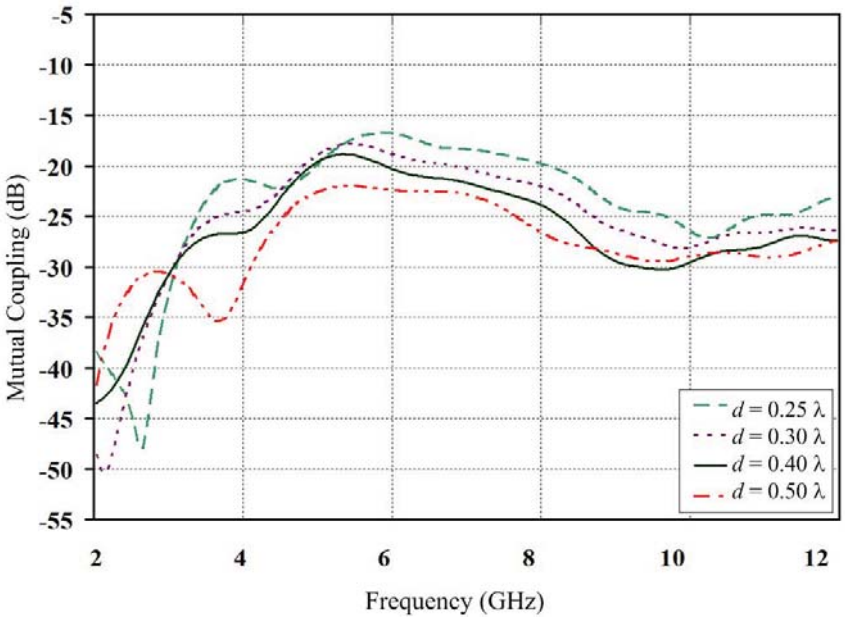

Figure 11. The simulation mutual coupling effect of orthogonal position when d is varied.

Fig. 10. After adjustment, appropriate value of d was 0.40λ at 6.85 GHz. If it was more than 0.50λ, the dimension of antenna structure would has a larger size. Fig. 11 shows the simulation comparison of the mutual coupling results of four different angular positions (seen in Figs. 9(a), (b), (c), and (d)). The simulation of orthogonal position achieved the values of mutual coupling lower than -18.88 dB.

3.2. Measurement and Simulation Results

The single port antenna was fabricated on the printed circuit board FR4 with a dimension of $34\times34\,\text{mm}^2$ as shown in Fig. 12(a). The orthogonal position of two ports antenna was fabricated with dimension of $34\times80\,\text{mm}^2$ as shown in Fig. 12(b). Consequently, the measurement results were achieved with Network Analyzer (E5071C). The comparison of simulation and measurement results of the reflection coefficient is shown in Fig. 13. The measurement results of the single port antenna were obtained in a frequency range of 2.72–12 GHz (126.53%) and two-port antenna at port1 of 2.84–12 GHz (123.45%). The mutual coupling of the two-port antenna was compared as seen in Fig. 14. It was found that the measurement results of mutual coupling were less than -22.5 dB.

The envelope correlation coefficient (ECC) is very important for MIMO communication systems. ECC (ρ_e) is related to the correlation between the antennas, and it affects the Signal-to-Noise Ratio

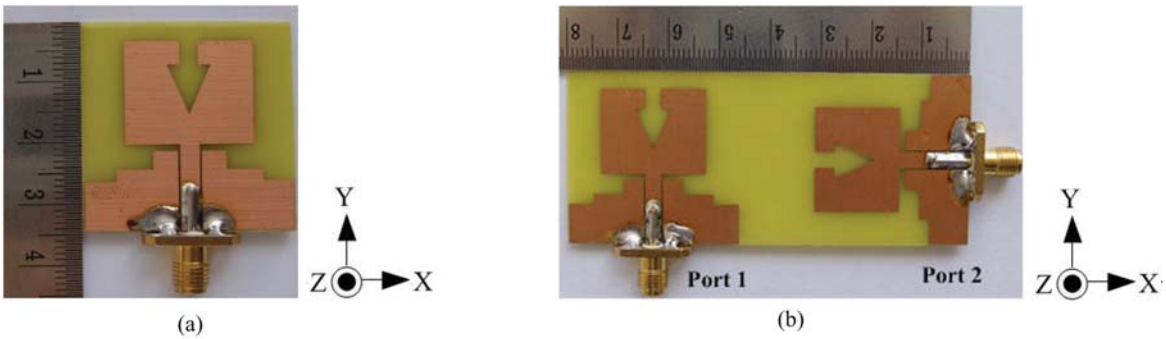

Figure 12. The fabricated antenna. (a) Single port antenna and (b) two port antenna.

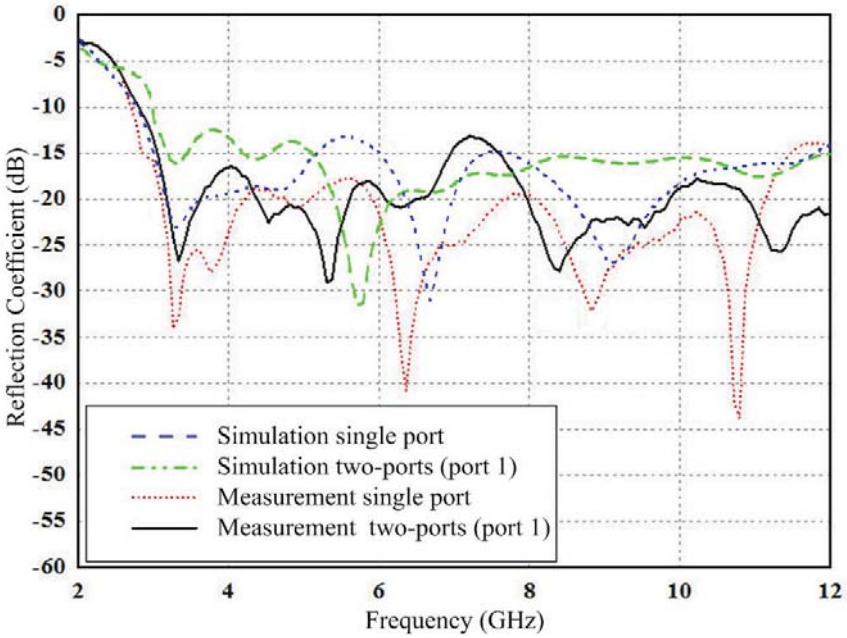

Figure 13. The comparison of simulation and measurement results of single port antenna.

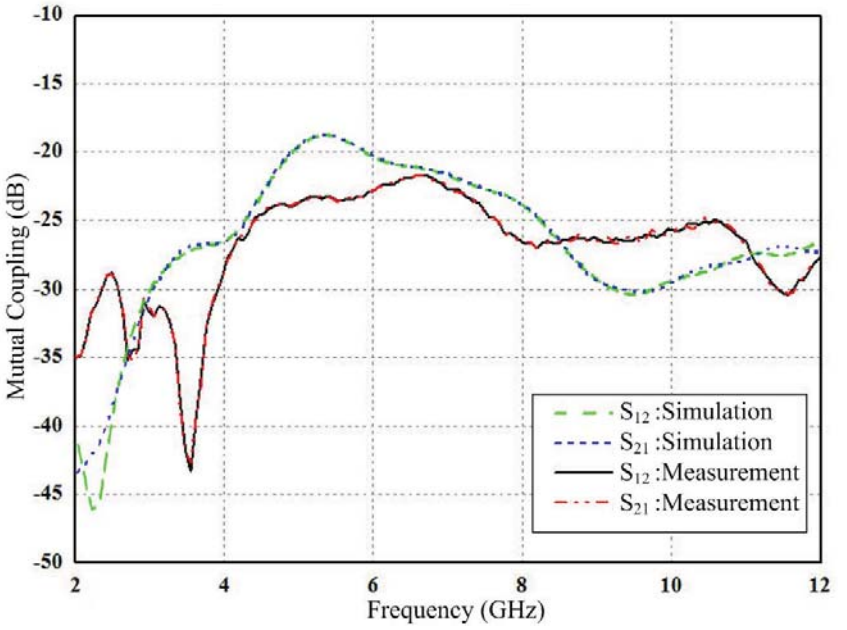

Figure 14. Comparison of simulation and measurement results of mutual coupling.

(SNR) of the system. The value as required for the UWB-MIMO antenna must be less than 0.5 [26]. The value of ECC can be calculated from the S-parameters [15, 24, 25] using the following Eq. (16). The comparison of ECC is shown in Fig. 15. The measurement result of ECC is lower than 0.001. The measurement result of group delay is good, lower than ± 2 ns as shown in Fig. 16.

$$\rho_e = \frac{\left|S_{11}^* S_{21} + S_{12}^* S_{22}\right|^2}{\left|\left(1 - \left|S_{11}\right|^2 - \left|S_{21}\right|^2\right)\left(1 - \left|S_{22}\right|^2 - \left|S_{12}\right|^2\right)\right|}, \tag{16}$$

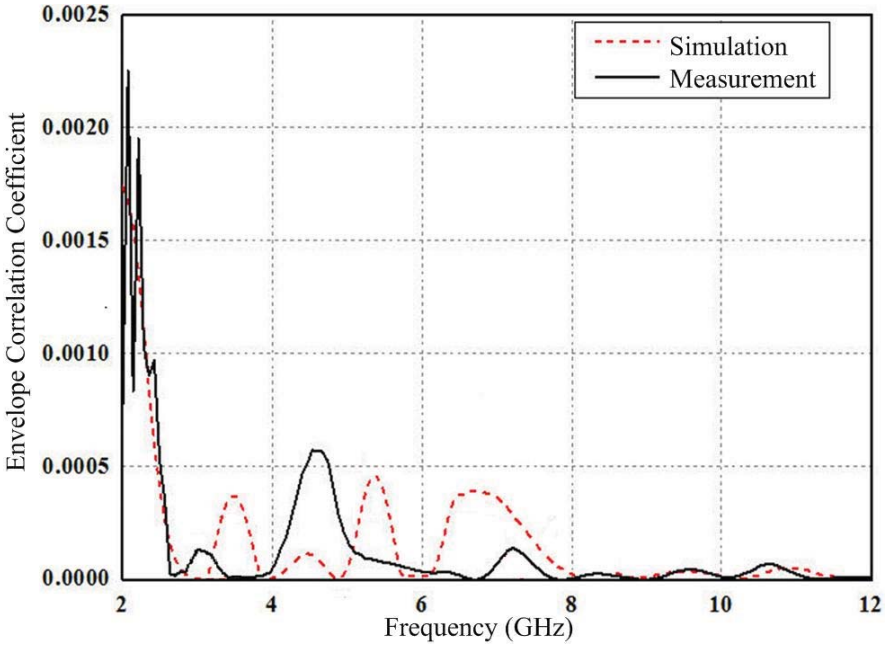

Figure 15. The comparison of envelope correlation coefficient (ρ_e).

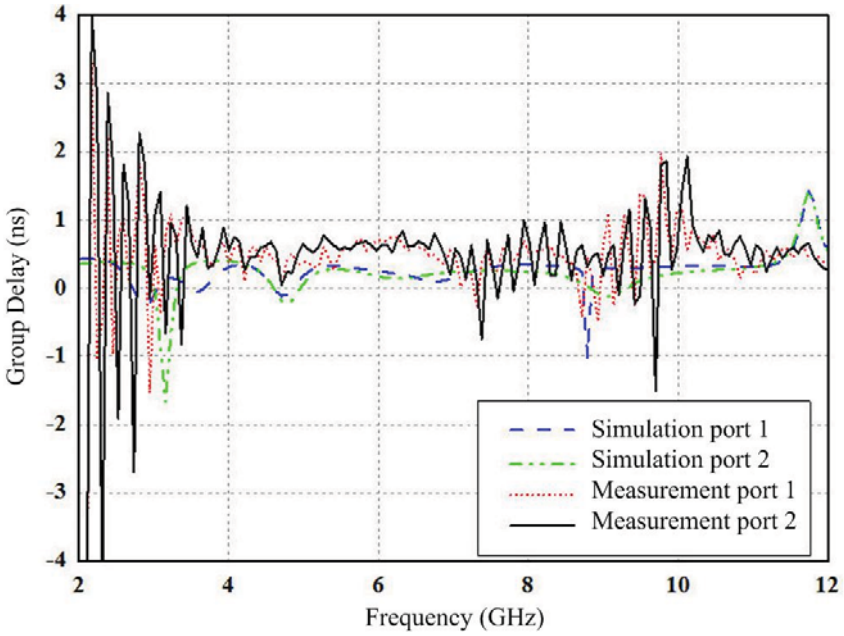

Figure 16. The comparison of group delay of two-port antenna.

4. FOUR PORT ANTENNA DESIGN

4.1. Four-Port Antenna Design

Finally, this paper proposes the four-port antenna. It is designed by placement difference without any structure between ports [9, 10, 15, 27]. In [13], the two-port antenna with orthogonal position produces the lowest mutual coupling and ECC. Then, the four-port antenna is redesigned. The dimensions of

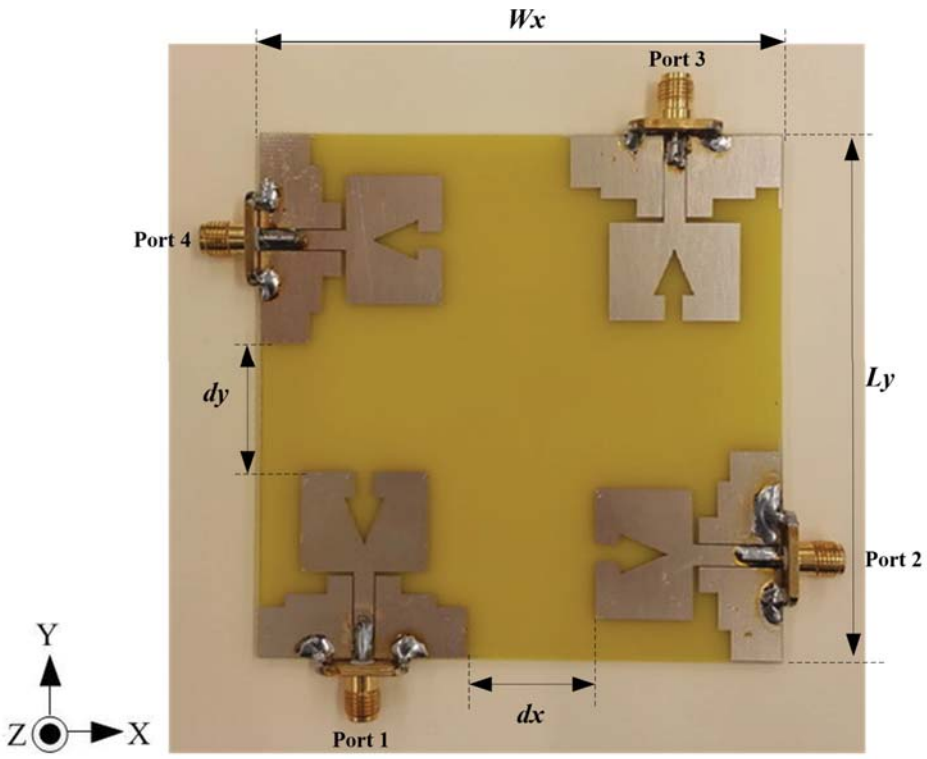

Figure 17. The fabricate prototype of four-port antenna.

fabricated four-port antenna are $W_x = L_y = 80\,\text{mm}$ and $d_x = d_y = 12\,\text{mm}$ as shown in Fig. 17.

The envelope correlation coefficient (ρ_e) of the proposed MIMO four-port antenna is calculated from multiple elements of antennas from S-parameters using Eq. (17) in [28].

$$\rho_e(i,j,N) = \frac{\left|\sum_{n=1}^{N} S_{i,n}^{*} S_{n,j}\right|^2}{\prod_{k=(i,j)} \left[1 - \sum_{n=1}^{N} S_{i,n}^{*} S_{n,k}\right]}, \tag{17}$$

Using Eq. (18), the envelope correlation coefficient between the antenna elements i and j in the (N, N) MIMO system can be calculated. When $i = 1$, $j = 2$, and $N = 4$, the envelope correlation of

Table 1. Comparison of reflection coefficient.

Port	Simulation		Measurement	
	Frequency (GHz)	BW %	Frequency (GHz)	BW %
1	2.70–12	126.53	2.60–11.06	123.87
2	2.70–12	126.53	2.49–10.67	124.32
3	2.70–12	126.53	2.65–11.20	123.58
4	2.70–12	126.53	2.87–11.10	117.88

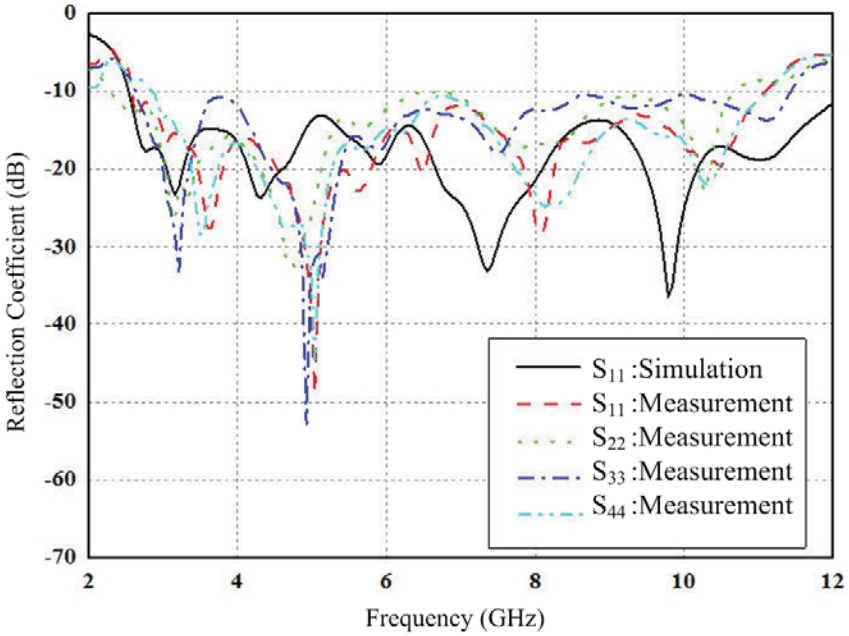

Figure 18. The comparison of simulation and measurement results of reflection coefficient.

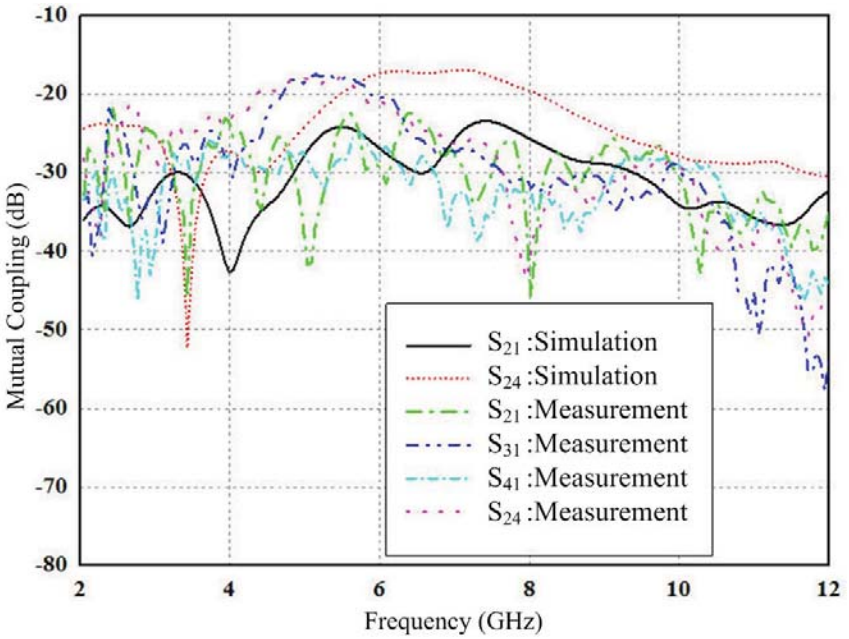

Figure 19. The measurement results of mutual coupling.

four-port MIMO antenna can be defined as Eq. (18).

$$\rho_e(1,2,4) = |S_{11}^* S_{12} + S_{12}^* S_{22} + S_{13}^* S_{32} + S_{14}^* S_{42}|^2 \times ([1 - (S_{11}^* S_{11} + S_{12}^* S_{21} + S_{13}^* S_{31} + S_{14}^* S_{41})] \times [1 - (S_{11}^* S_{12} + S_{12}^* S_{22} + S_{13}^* S_{32} + S_{14}^* S_{42})])^{-1} \quad (18)$$

4.2. Measurement and Simulation Results of Four Port Antenna

The prototype of the four-port antenna is fabricated with a dimension of $80 \times 80\,\text{mm}^2$ as shown in Fig. 17. The simulation and measurement results of the reflection coefficient are shown in Table 1 and compared in Fig. 18. The measurement results of the reflection coefficient cover the bandwidth of 3.1–10.6 GHz for UWB-MIMO antenna.

In terms of ECC, the measurement system of the ECC was installed with four-ports of the proposed

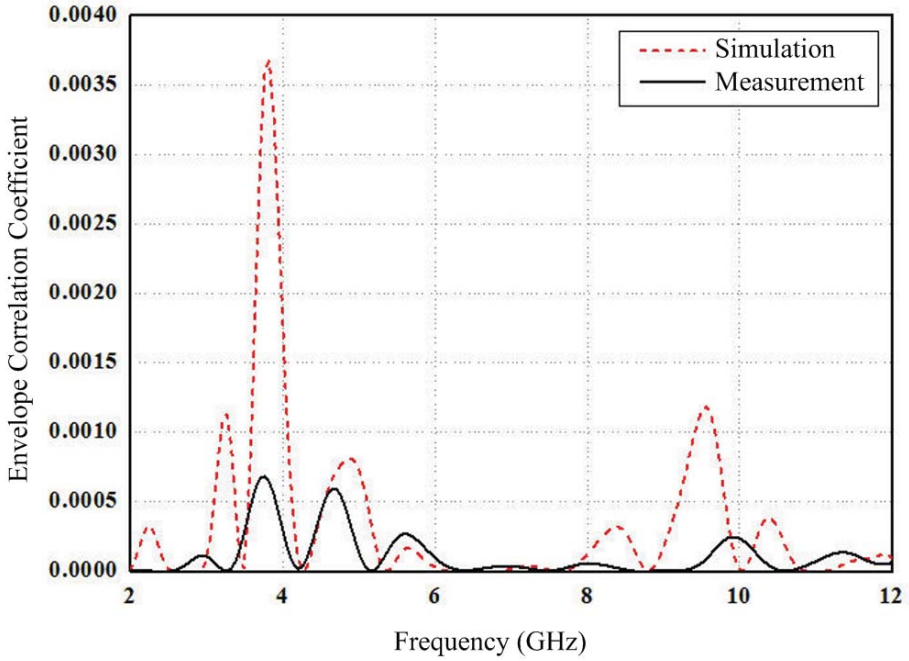

Figure 20. The envelope correlation coefficient.

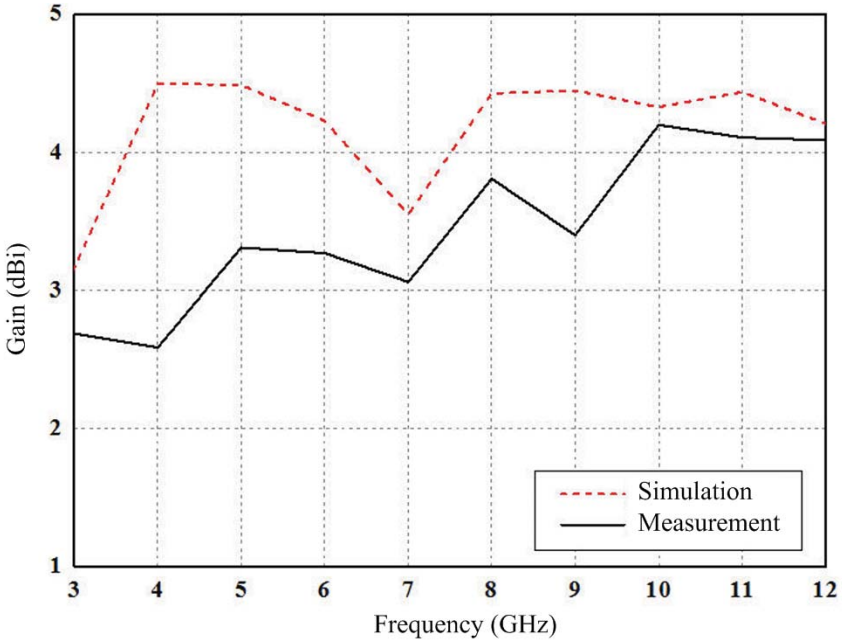

Figure 21. The simulation and measurement results of the gain.

antenna to transmit and receive. At that time, the transmission and reflection efficiencies were noted as S_{11}, S_{22}, S_{33}, S_{44}, S_{12}, S_{13}, S_{14}, S_{23}, and S_{34}. Finally, the ECC was calculated by Eq. (18). Fig. 19 shows the comparison of simulation and measurement results of mutual coupling. It was observed that the lowest value of the measurement result was lower than -17.4 dB and better than the simulation results. The simulation and measurement results of ECC (ρ_ε) are calculated by Eq. (18), and the comparison results are shown in Fig. 20. It was noticed that the simulation result was lower than 0.004. Also, the measurement result was lower than 0.001. The simulation and measurement results are 3.99 dBi and 3.38 dBi, respectively, and the average gain is at 3–12 GHz as shown in Fig. 21. Considering the measurement results, the measured gain was lower than the simulated result at low frequency due to the use of lead in soldering the SMA connector with the FR4 plate, so the electrical conductivity was exacted. The radiation patterns of simulation and measurement results of E-plane and H-plane of 3.1 GHz, 7 GHz and 10.6 GHz are shown in Fig. 22 and Fig. 23, respectively. According to the results, it is found that the simulated radiation patterns are in good agreement with measured one which are bi-directional patterns.

The efficiency of the four-port rectangular monopole antenna is compared as seen in Fig. 24. It

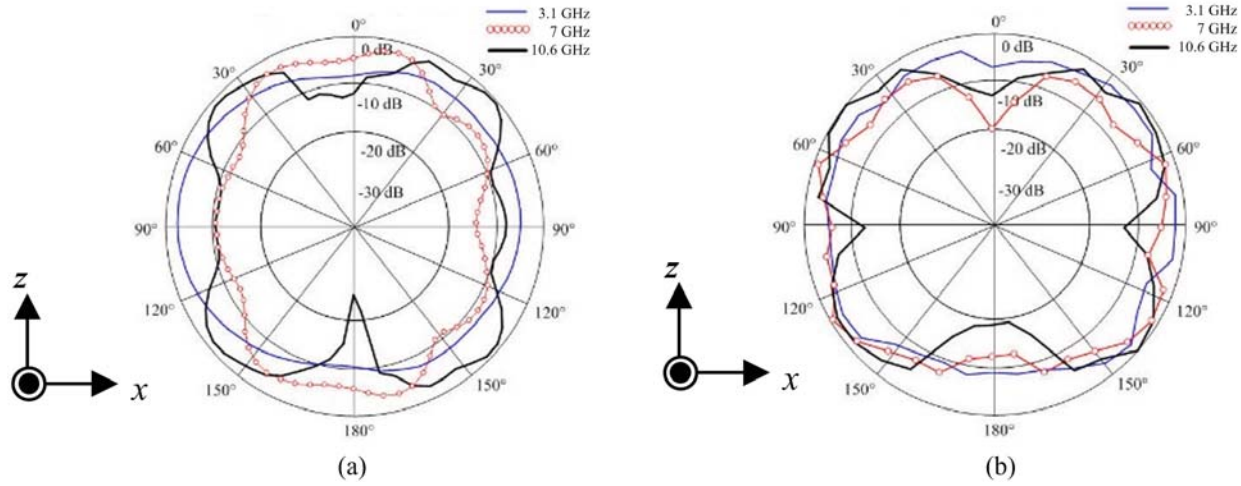

Figure 22. The radiation patterns of simulation and measurement results of E-plane. (a) Simulation. (b) Measurement.

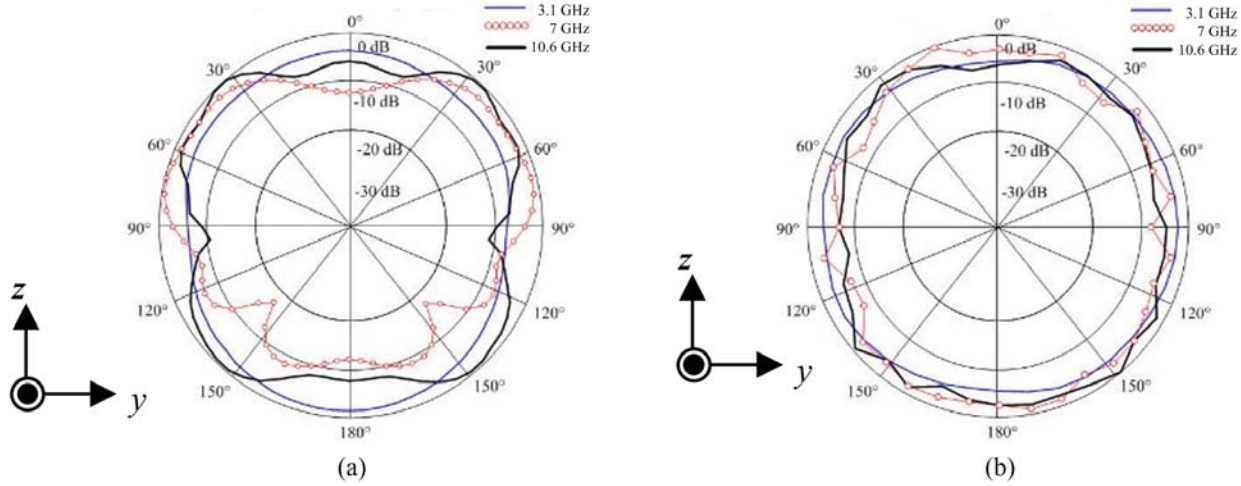

Figure 23. The radiation patterns of simulation and measurement results of H-plane. (a) Simulation. (b) Measurement.

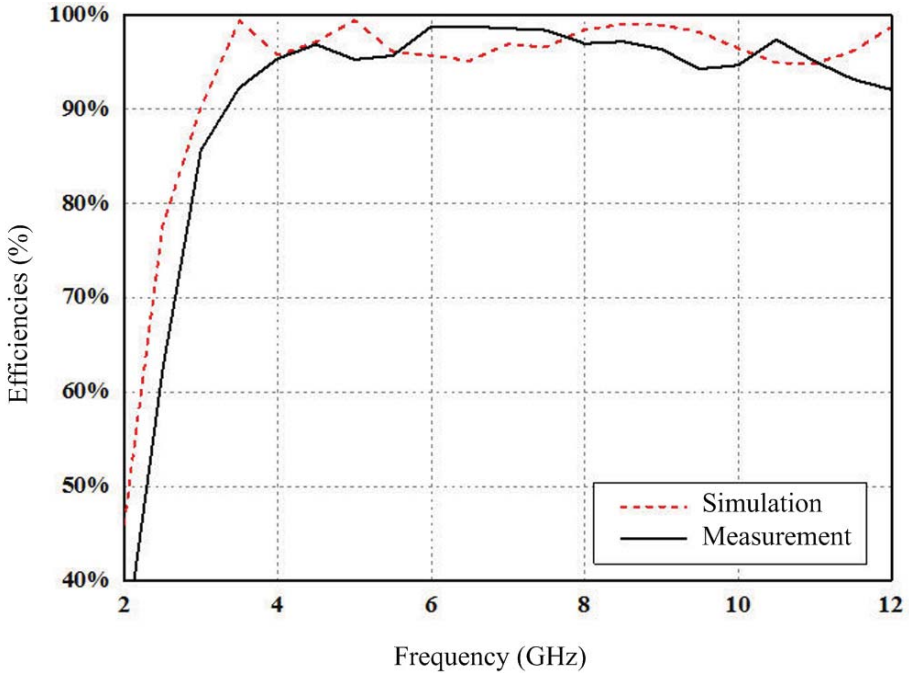

Figure 24. The simulation and measurement results of efficiency.

can be observed that the measurement of efficiency is more than 85.70%. It is acceptable in the UWB-MIMO antenna. The measurement system of radiation efficiency of the antenna was set up with a tapered slot antenna to transmit the signal with transmitting power of 0 dB (Pt), and the proposed one port antenna acted as the receiver (receiving power: Pr). Therefore, the antenna efficiency can be calculated as follows, and the radiation efficiency in actual operation is always below 100% (0 dB). The antenna efficiency was measured in the chamber room by feeding some power to the feed point of the

Table 2. Comparison of efficiency of the proposed antenna with the previous researches.

Reference	Frequency Band (GHz)	Ports	Antenna size (mm^3)	Isolation (dB)	ECC	Gain	Efficiency (%)
[29]	2–10.6	4	45×45	> 17	< 0.005	3.5	-
[30]	3–16.2	4	60×60	17.5	< 0.3	8	91.2
[31]	3.1–10.6	4	32×36	> 20	< 0.0025	-	60
[32]	3.0–15.0	4	38×38	> 15	< 0.15	0.5–5.0	-
[33]	3.1–10.6	4	50×28	18	< 0.12	-	-
[34]	3.1–11	4	40×40	> 20	< 0.01	1.3–4.0	-
[35]	1.77–2.51	4	120×60	13	< 0.248	3.2	75
[36]	3.1–10.6	4	100×100	> 20	< 0.1	-	-
[37]	2.3–13.75	4	39×39	> 22	< 0.02	1.4–4.6	-
[38]	3.1–10.6	4	40×43	20	< 0.2	4	92
[39]	4.8–7.7	4	81×87	> 20	< 0.1	4–8.48	-
[40]	2.5–12	4	37×46	> 20	< 0.005	4	80
Proposed	2.6–11	4	80×80	-17.4	< 0.001	3.38	85.70

antenna and measuring the strength of the radiated electromagnetic field in the surrounding space. A good UWB-MIMO antenna must radiate more than 80% of the energy fed to it [15].

The efficiency of the four-port rectangular monopole antenna is compared as seen in Fig. 24. It can be observed that measurement of the efficiency is more than 85.70%. It is acceptable in a UWB-MIMO antenna. The envelope correlation coefficient for the MIMO system is obtained under 0.001 which is less than the specific parameters of UWB-MIMO antennas. The radiation pattern is bi-directional. Also, the efficiency of the four-port antenna is more than 85.70%. In Table 2, the summarization of the efficiency property of proposed UWB-MIMO antennas is compared to the previous research.

5. CONCLUSIONS

A four-port rectangular monopole antenna for UWB-MIMO applications is presented in this paper. The proposed antennas were designed by using step etching on the ground plane and arrow-shaped slot etching on the radiating patch to enhance bandwidth and improve performance. The advantages of using the arrow-shaped slot etching technique are: reduced group delay in sending pulse signals making it more efficient or more accurate, and it reduces the distance classified to less than 0.50λ, which decreases to 0.40λ, at 6.85 GHz. The homogeneous elements and angular variation techniques can be applied to reduce the effect of correlation between multiple antenna elements keeping the dimension structure unchanged. The proposed antenna was designed by placement in the orthogonal position. The measurement results found that coverage of the frequency was in the range of 3.1–10.6 GHz as defined by an FCC for UWB communications, a low mutual coupling of less than −17.4 dB, the envelope correlation coefficient less than 0.001 in the specific parameter of UWB-MIMO antenna, bi-directional pattern, and an average gain of 3.38 dBi. Also, the efficiency of the four-port rectangular monopole antenna was more than 85.70%. The benefits of the above mentioned antenna can be used to communicate with wireless networks on the human body to find abnormalities in the body or to detect various diseases within the body using frequency waves or medical devices that need precision in surgery or being 100% accurate. It can actually reduce the time of operation and in finding the position of moving objects with accuracy up to a centimeter in a hazardous area or a chemical area, etc.

ACKNOWLEDGMENT

The authors would like to thank the department of Telecommunications Engineering, Faculty of Engineering and Architecture, Rajamangala University of Technology Isan (RMUTI) for supporting this research with equipment and funding. Moreover, the authors gratefully acknowledge the simulation CST software for its support as well as the School of Telecommunication Engineering, Suranaree University of Technology, Nakhonratchasima, Thailand; for the sponsorship.

REFERENCES

1. Raut, P. and S. Badjate, "MIMO-future wireless communication," *International Journal of Innovative Technology and Exploring Engineering (IJITEE)*, Vol. 2, No. 5, 102–106, 2013.
2. Wang, Z., L. Liu, J. Cai, Z. Shao, Y. Yang, and X. Zhu, "2.4 GHz/5 GHz wide-band receiver in a wireless communication system based on 4×4 MIMO technology," *2012 International Conference on Computational Problem-Solving (ICCP)*, 182–185, 2012.
3. Kim, S.-H., J.-Y. Lee, T. T. Nguyen, and J.-H. Jang, "High-performance MIMO antenna with 1-D EBG ground structures for handset application," *IEEE Antennas and Wireless Propagation Letters*, Vol. 12, 1468–1471, 2013.
4. Jiang, X., H. Wang, and T. Jiang, "A low mutual coupling MIMO antenna using EBG structures," *2017 Progress In Electromagnetics Research Symposium — Spring (PIERS)*, Vol. 12, 660–663, St. Petersburg, Russia, May 22–25, 2017.
5. Sun, Y., Q. Huang, and X. Shi, "A low mutual coupling MIMO antenna using EBG structures," *2016 IEEE International Conference on Microwave and Millimeter Wave Technology (ICMMT)*, Vol. 2, 701–703, 2016.

6. Numan, A.-B., M.-S. Sharawi, A. Steffes, and D.-N. Aloi, "A defected ground structure for isolation enhancement in a printed MIMO antenna system," *2013 7th European Conference on Antennas and Propagation (EuCAP)*, 2123–2126, 2013.
7. Jusoh, M., M. F. B. Jamlos, M. R. Kamarudin, and M. F. B. A. Malek, "A MIMO antenna design challenges for UWB application," *Progress In Electromagnetics Research*, Vol. 36, 357–371, 2012.
8. Rakluea, P. and P. Poch, "Development of circular ring antennas for mobile broadband systems," *2015 7th International Conference on Information Technology and Electrical Engineering (ICITEE)*, 530–533, 2015.
9. Najam, A. I., Y. Duroc, and S. Tedjini, "Design and analysis of MIMO antennas for UWB communications," *Proceedings of the Fourth European Conference on Antennas and Propagation*, 1–5, 2010.
10. Jusoh, M., M. F. Jamlos, M. F. Malek, M. R. Kamarudin, and H. Harun, "Analysis of radiation efficiency effects on UWB MIMO tree-antenna positioning," *2012 Asia-Pacific Symposium on Electromagnetic Compatibility*, 897–900, 2012.

11. Dao, M.-T., V.-A. Nguyen, Y.-T. Im, S.-O. Park, and G. Yoon, "3D polarized channel modeling and performance comparison of MIMO antenna configurations with different polarizations," *IEEE Transactions on Antennas and Propagation*, Vol. 59, No. 7, 2672–2682, 2011.
12. Kumar, R. and N. Pazare, "Compact printed ultra-wideband diversity monopole antenna with slantinverted tree-shaped stub," *IET Microwaves, Antennas & Propagation*, Vol. 9, No. 14, 1595–1604, 2015.
13. Naktong, W., S. Kornsing, P. Boonmaitree, P. Dabbung, and A. Ruengwaree, "Study of geometryshaped monopole antenna with step-shaped etching technique on ground plane," *2016 13th International Conference on Electrical Engineering/Electronics, Computer, Telecommunications and Information Technology (ECTI-CON)*, 1–4, 2016.
14. Saad-Bin-Alam, Md., M. S. Ullah, and S. Moury, "Design of a narrowband 2.45 GHz unidirectional microstrip antenna with a reversed 'Arrow' shaped slot for fixed RFID tag and reader," *2013 2nd International Conference on Advances in Electrical Engineering (ICAEE)*, 301–304, 2013.
15. Thongbor, P., A. Ruengwaree, V. Pirajnanchai, W. Naktong, and N. Fhafhiem, "Rectangular monopole antenna with arrow-shaped slot etching for UWB-MIMO application," *2016 13th International Conference on Electrical Engineering/Electronics, Computer, Telecommunications and Information Technology (ECTI-CON)*, 1–4, 2016.
16. Werfelli, H., K. Tayari, M. Chaoui, M. Lahiani, and H. Ghariani, "Design of rectangular microstrip patch antenna," *2016 2nd International Conference on Advanced Technologies for Signal and Image Processing (ATSIP)*, 798–803, 2016.
17. Balanis, C. A., *Antenna Theory: Analysis and Design*, John Wiley & Sons, 2016.
18. Yadav, M. B., B. Singh, and V. S. Melkeri, "Design of rectangular microstrip patch antenna with DGS at 2.45 GHz," *2017 International Conference of Electronics, Communication and Aerospace Technology (ICECA)*, Vol. 1, 2017.
19. Simons, R. N., *Coplanar Waveguide Circuits, Components, and Systems*, Vol. 165, 367–370, John Wiley & Sons, 2004.
20. Li, X. F., "Design of a CPW-fed wideband planar monopole antenna with omni-directional pattern improvement," *2015 IEEE International Conference on Communication Problem-Solving (ICCP)*, 271–273, 2015.
21. Federal Communications Commission, "Revision of part 15 of the commission's rules regarding ultra-wideband transmission systems: First report and order," FCC 02.V48, April 2002.
22. Jan, J.-Y., J.-C. Kao, Y.-T. Cheng, W.-S. Chen, and H.-M. Chen, "CPW-fed wideband printed planar monopole antenna for ultra-wideband operation," *2006 IEEE Antennas and Propagation Society International Symposium*, Vol. 59, No. 7, 1697–1700, 2006.
23. Yoon, H. K., W. S. Kang, Y.-J. Yoon, and C.-H. Lee, "A CPW-fed flexible monopole antenna for UWB systems," *2007 IEEE Antennas and Propagation Society International Symposium*, 701–704, 2007.
24. Matin, M. A., "Ultra wideband: Current status and future trends," *BoD — Books on Demand*, 2012.
25. Manteuffel, D., "MIMO antenna design challenges," *2009 Loughborough Antennas & Propagation Conference*, 50–56, 2009.
26. Vaughan, R. G. and J. B. Andersen, "Antenna diversity in mobile communications," *IEEE Transactions on Vehicular Technology*, Vol. 36, No. 4, 149–172, 1987.
27. Najam, A. I., Y. Duroc, and S. Tedjini, "A four-element Ultra Wideband (UWB) diversity antenna," *2010 IEEE Antennas and Propagation Society International Symposium*, 1–4, 2010.
28. Dama, Y., A. S. Hussaini, R. A. Abd-Alhameed, S. M. R. Jones, N. J. McEwan, T. Sadeghpour, and J. Rodriguez, "Envelope correlation formula for (N, N) MIMO antenna array including power losses," *2011 18th IEEE International Conference on Electronics, Circuits, and Systems*, 508–511, 2011.
29. Tripathi, S., A. Mohan, and S. Yadav, "A compact Koch fractal UWB MIMO antenna with WLAN band-rejection," *IEEE Antennas and Wireless Propagation Letters*, Vol. 14, 1565–1568, 2015.

30. Wu, W., B. Yuan, and A. Wu, "A quad-element UWB-MIMO antenna with band-notch and reduced mutual coupling based on EBG structures," *International Journal of Antennas and Propagation*, Vol. 2018, Article ID 8490740, 10 pages, 2018.
31. Muhammad, B., S. Rashid, A. Hammad, S. Muhammad Farhan, and B. Anthony, "An FSS-based nonplanar quad-element UWB-MIMO antenna system," *IEEE Antennas and Wireless Propagation Letters*, Vol. 16, 987–990, 2016.
32. Deepika, S., A. Mahesh, and K. Shiban Kishen, "Easily extendable compact planar UWB MIMO antenna array," *IEEE Antennas and Wireless Propagation Letters*, Vol. 16, 2328–2331, 2017.
33. Ahmed, I., M. Jan, and S. Raed, "Compact UWB MIMO antenna with pattern diversity and band rejection characteristics," *Microwave and Optical Technology Letters*, Vol. 59, No. 6, 1460–1464, 2017.
34. Wael, A. E. A. and I. Ahmed, "A compact double-sided MIMO antenna with an improved isolation for UWB applications," *AEU — International Journal of Electronics and Communications*, Vol. 82, 7–13, 2017.
35. Rifaqat, H., S. Mohammad, and S. Atif, "An integrated four-element slot-based MIMO and a UWB sensing antenna system for CR platforms," *IEEE Transactions on Antennas and Propagation*, Vol. 66, No. 2, 978–983, 2017.
36. Mohamed, S., S. Mohamed Sameh, and M. Hassan, "Dual notched band quad-element MIMO antenna with multitone interference suppression for IR-UWB wireless applications," *IEEE Transactions on Antennas and Propagation*, Vol. 66, No. 11, 5737–5746, 2018.
37. Tang, Z., X. Wu, J. Zhan, S. Hu, Z. Xi, and Y. Liu, "Compact UWB-MIMO antenna with high isolation and triple band-notched characteristics," *Applied Sciences*, Vol. 7, 19856–19865, 2019.
38. Fatima, A., S. Rashid, S. Tayyab, B. Muhammad, and S. Farhan, "A compact quad-element UWB-MIMO antenna system with parasitic decoupling mechanism," *Applied Sciences*, Vol. 9, No. 11, 2371, 2019.
39. Kunal, S., K. Ashwani, K. Binod, D. Santanu, and K. Sachin, "A CPW-fed UWB MIMO antenna with integrated GSM band and dual band notches," *International Journal of RF and Microwave Computer-Aided Engineering*, Vol. 29, No. 1, e21433, 2019.
40. Kamel Salah, S. and A. Haythem Hussein, "Planar UWB MIMO-diversity antenna with dual notch characteristics," *Progress In Electromagnetics Research C*, Vol. 93, 119–129, 2019.